Low Reynolds Number Flow Around a Flying Saucer Micro Air Vehicle

S. Cortés[1], D. Güemes[*2], R. Ávila[3]
[1]Universidad Nacional Autónoma de México, [2]Universidad Nacional Autónoma de México,
[3]Universidad Nacional Autónoma de México
*Departamento de Termofluidos, Facultad de Ingeniería, Universidad Nacional Autónoma de México, D.F. C.P. 04510, daguov_39@yahoo.com .mx

Abstract: Today Unmanned Air Vehicles (UAV) are a reality, nonetheless the tendency of these devices is to decrease their size in order to produce stealthy and undetectable vehicles. The purpose of this paper is to analyze the behavior during flight of a small scale UAV. This device has the shape of a flying saucer with dimensions: 4.2885 mm high and 10 mm wide. In order to achieve our goal, we performed two simpler analyses which consisted on the simulation of a flow around a cylinder in 2D and around a sphere in 3D for different Reynolds number. These analyzes were performed in order to compare the results to those found in the literature.

Keywords: Flow around, two-dimensional bodies, three-dimensional bodies, drag coefficient, lift coefficient, Reynolds number, flying saucer.

1. Introduction

This paper aims to the understanding of the aerodynamics of a Nano Air Vehicle (NAV). In order to accomplish this goal, we proposed two hypotheses.

Our first hypothesis was that our device flies in very large spaces, therefore, for the simulation we considered a large domain. Our second hypothesis was that the speed developed by the vehicle is very low. Taking into account these considerations, we obtained as results the drag and lift coefficients and the velocity field around the NAV.

2. Equations

This paper is a study related with the movement of a fluid and the interaction this fluid has with a solid body without considering the heat transfer between the two. The equations governing this type of analysis are the *mass conservation equation.*

$$\nabla \cdot V = 0$$

and the Navier-Stokes equation:

$$\rho\left(\frac{\partial V}{\partial t} + V \cdot \nabla V\right) = -\nabla P + \eta \nabla^2 V + \rho F$$

3. Flow around a cylinder

The study of a flow around a circular cylinder is a basic problem in fluid mechanics. The flow pattern around the cylinder depends on the Reynolds number, which in this case is defined as:

$$Re_D = \frac{\rho U_\infty D}{\mu}.$$

In terms of this parameter we have the following description of the phenomenology of the flow. When the range is between $1<Re_D<20$, the viscous forces control the flow and this is reflected in the fluid attaching onto the surface of the cylinder. When $Re_D \approx 20$, the flow behind the cylinder becomes a pair of stationary vortices whose length depends on Re_D[1].

For values of $Re_D > 100$, the vortices become unstable and begin to vibrate irregularly and finally shedding alternately on both sides of the symmetry axis periodically as shown in Fig. 1.

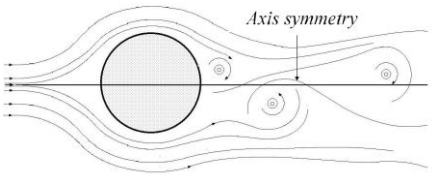

Figure 1. Two-dimensional flow around a cylinder $Re_D > 100$

The shedding frequency of the vortices is related to the flow velocity by the Strouhal number defined as:

$$St = \frac{fD}{U_\infty}$$

Moreover, the forces caused by the fluid motion around the cylinder can be analyzed (lift and drag forces). This analysis can be performed by dimensional numbers such as the lift and drag coefficients. The drag coefficient (C_D) can be calculated as:

$$C_D = \frac{F_D}{\frac{1}{2}\rho A_p U_\infty^2}.$$

3.1 Cases of study

Six different simulations were performed, each of them corresponding to a different Reynolds number. This was made with the purpose of comparing the drag coefficient (C_D) obtained from the simulations with the ones found in literature.

The size of the domain used for the first simulations was the one proposed by Li [2], shown in Fig. 2. Unfortunately, the results with this domain weren't satisfactory. In the work of Piñol and Grau [3], we can appreciate that the dimensions of the domain affect the results of the simulations. For this reason we decided to change them, as well as the position of the center of the cylinder to obtain better results, as shown in Table 1.

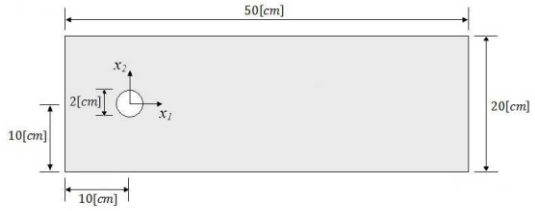

Figure 2. Dimensions proposed by Li [2]. These dimensions were considered for the study.

Reynolds number	Width of the domain (cm)	Length of the domain (cm)	Distance between the center of the cylinder and the origin. (cm)
31.25	9	50	-6.5
59.375	9.5	50	-6.5
78.125	20	50	-5
90.6	17	50	-5
100	17.5	50	-5
312.5	18.8	51.8	0.57

Table 1. Dimensions of the domain for the different analyses performed.

3.2 Analysis of the problem using COMSOL.

In the literature we can find that these types of analyses are performed in steady state due to the nature of the phenomenon. For values of $Re_D > 100$ behind the cylinder a von Kármán wake of vortices is formed. Therefore, this analysis is time dependant [4].

The boundary conditions were: input speed (U_∞) on the left side, the right wall represents the output with a reference pressure of 0, finally, symmetry conditions on the upper and lower walls.

The fluid chosen for this analysis was air at 25º C and pressure of 1 atm. The properties of this fluid for the simulation were: density of 1.184 kg/m^3 and dynamic viscosity of 1.849×10^{-5} N s/m^2.

3.2.1 Computational grid

The computational grid consisted on triangular elements, while on the cylinder's surface we had a finer grid in comparison to the rest of the domain as shown in Fig 3. The total number of elements for this grid can be seen in Table 2.

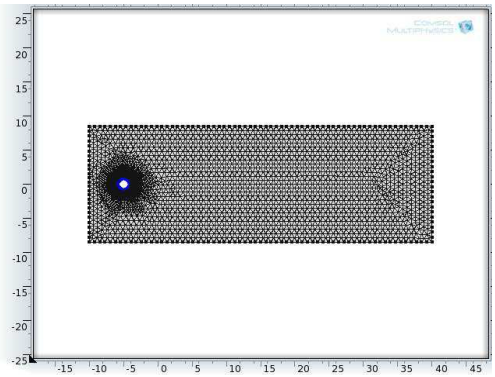

Figure 3. Computational grid in the domain.

5. Creating the PDF

Reynolds	Number of elements within the grid.
31.25	17376
59.375	16788
78.125	8690
100	8474
312.5	9966

Table 2. Number of elements in the grid for each simulation.

3.2.2 Results.

The velocity field obtained from the simulations for the range between 31.25<Re_D<100 is adjusted to the one described in literature as shown in Fig 4. In the simulation corresponding to Re_D=312.5, shown in Fig 5, we can observe the shedding of the vortices.

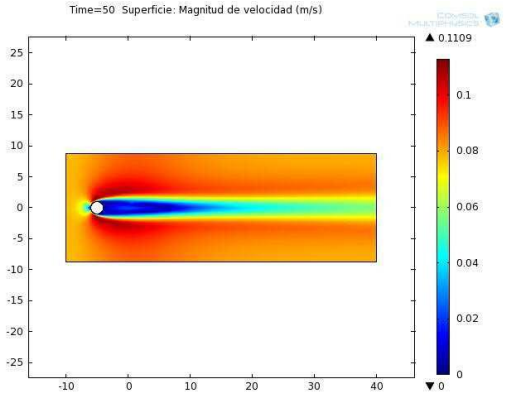

Figure 4. Velocity field around the cylinder when Re_D=100.

The drag coefficient (C_D) was one of the parameters calculated as part of the results obtained from the simulations of this study. Table 3 shows the drag coefficient for each simulation, as well as those reported in the literature.

Reynolds	C_D measured in the simulations	C_D shown in literature	Percentage error
31.25	2.937875	2.903	1.2
59.375	2.252767	2.258	0.232
78.125	1.609433	1.6129	0.215
90.6	1.551598	1.5564	0.308
100	1.501333	1.5	0.089
312.5	1.4225	1.3225	7.561

Table 3. Comparison of the drag coefficient obtained by COMSOL and the ones obtained from the literature.

The Strouhal number reported in the literature for Re_D=312.5 is of 0.2026 and the one obtained from the simulation was of 0.20491981. The absolute error associated to these values is 2.3108×10^{-3} and the percentage error is of 1.14%.

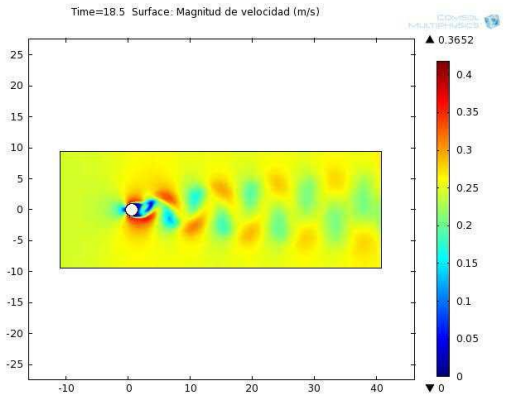

Figure 5. Shedding of the vortices when Re_D=312.5.

4. Flow around a sphere

The flow around a sphere is more difficult to understand due to its three-dimensional nature. Taneda [5] in the 50's performed several experiments in the range between 5<Re_D<300. In these works we can observe that the fluid remains attached to the surface of the sphere until $Re_D \approx 24$ is reached, as shown in Fig. 6.

Figure 6. Image obtained by Taneda [5] for Re_D=73.6.

For a Re_D >24 a pair of stationary vortices behind the sphere are formed and these vortices grow until they reach a Re_D=130. When Re_D>130 the wake produced by the vortices becomes unstable causing a slight periodic motion as shown in Fig. 7.

(a) Schematic of the flow around a sphere

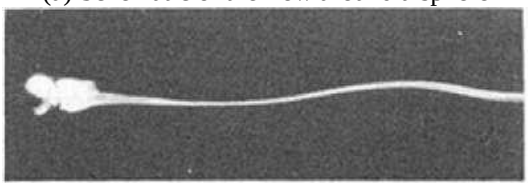

(b) Photograph of the flow around a sphere

Figure 7. Stationary vortices behind a sphere 130<Re_D<210 [6]

4.1 Cases of study

For this study, five different simulations were performed in the range 30 <Re_D< 210. The dimensions of the domain for this study were taken from the work presented by Defraeye, Verboven y Nicolai [7] shown in Fig 8. The diameter of the sphere was of 2 cm.

The results obtained with the domain shown in Fig 8 were unacceptable. As in the analysis performed for the cylinder, the dimensions of the domain for this analysis were modified, as well as the position of the sphere, until satisfactory results were achieved. Table 4 shows the dimensions of the domain for each analysis.

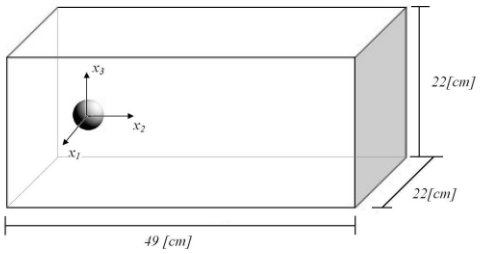

Figure 8. Original dimensions of the domain

Reynolds	Width of the domain (cm).	Length of the domain (cm).	Distance between the center of the sphere and the origin (cm)
32.25	3	25	-9.5
59.375	3	25	-9
78.125	3	25	-8.5
90.625	3	25	-6.5
206.5	3	25	-6.5

Table 4. Dimensions of the domain for the different analysis performed for the flow around a sphere.

4.2 Analysis of the problem using COMSOL.

The numerical experiments performed with COMSOL were, like the analysis for the flow around a cylinder, time dependant. The boundary conditions are shown in Fig. 9.

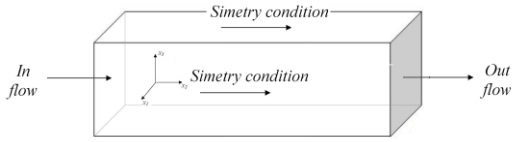

Figure 9. Boundary conditions for the analysis of flow around a sphere.

The fluid used for this analysis was water at 5º C, density of 1000 kg/m3 and dynamic viscosity of 1.518×10-3 N s/m^2.

4.2.1 Computational grid.

The computational grid consisted on tetrahedral elements as shown in Fig 10. Table 5 shows the number of elements in the grid for each analysis.

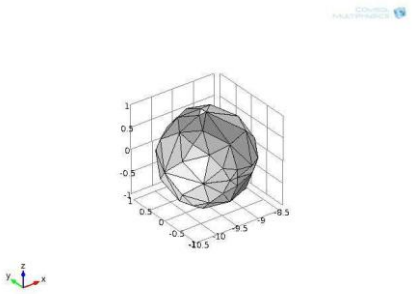

(a) Elements that compose the surface of the sphere

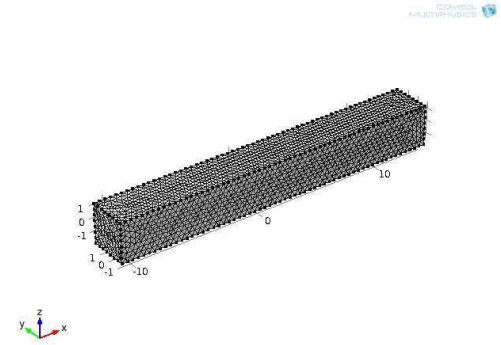

(b) Elements that compose the domain.

Figure 10. Grid that composes the domain.

Reynolds	Number of elements around the surface of the sphere	Number of elements in the domain.
32.25	120	47917
59.375	120	48239
78.125	120	48201
90.625	120	48412
206.5	120	48412

Table 5. Number of elements that compose the domain for each analysis.

4.2.2 Results

The obtained results for these analyses were the velocity fields and the drag coefficient. Fig. 11 shows the velocity field in 3D. This image shows the constant speed surfaces.

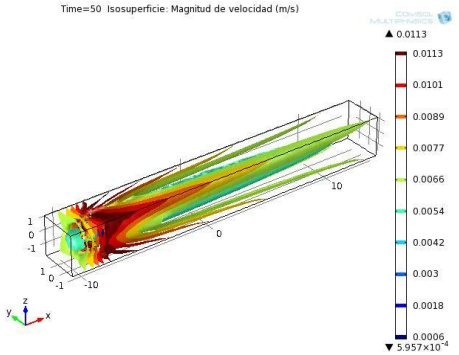

Figure 11. 3D velocity field for $Re_D = 78.125$.

Fig 12 shows the velocity field in 2D. This image shows in detail the direction of the velocity field in the middle plane of the sphere.

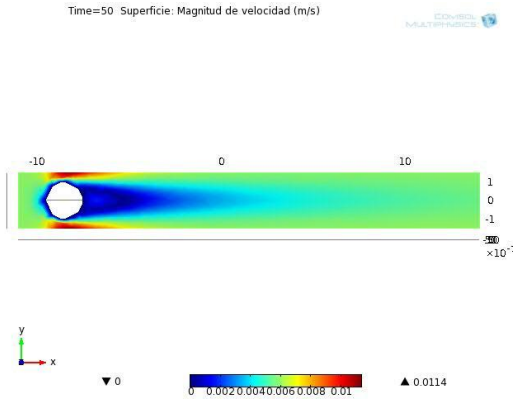

Figure 12. 2D velocity field for $Re_D = 78.125$.

The comparison between the drag coefficient obtained by the simulation and the ones found in the literature are shown in Table 6.

Reynolds	C_D obtained from the simulation	C_D found in the literature	Percentage error
32.25	2.44299	2.445	0.082
59.375	1.62162	1.623	0.085
78.125	1.47706	1.48	0.199
90.625	1.37277	1.3728	0.002
206.5	1.36427	1.3649	0.005

Table 6. Comparison of the drag coefficient obtained by COMSOL and the ones obtained from the literature.

5. Analysis of the flow around a flying saucer

The experimental analysis of complex three-dimensional geometries is very difficult to carry

out; therefore a simulation was performed for a small flying saucer.

As it is a very odd geometry, there are no reference for the drag and lift coefficients, hence the present study to obtain these parameters, as well as the velocity field.

5.2 Case of study

The analyzed air vehicle has a very small size. Its dimensions are: 4.2885 mm high and 10 mm wide as shown in Fig 13.

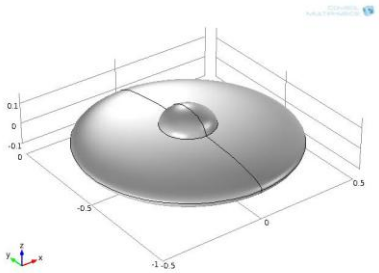

Figure 13. Prototype analyzed.

Because it is a small object, the speed which it can be subjected is very low; therefore the Reynolds number was equal to 497.57. The domain for this analysis was a rectangle with the following dimensions: 8 cm wide, 30 cm in length and 4 cm high.

5.2 Analysis of the problem using COMSOL.

The boundary conditions used for this analysis were the same as shown in Fig 9, that is, an input is declared with a normal speed with a value of 0.5 m/s, an output with a reference pressure equal to 0 and symmetry conditions on the sides of the domain.

The fluid for this analysis was air at 25º C and pressure of 1 atm. The properties of this fluid for the simulation were: density of 1.184 kg/m^3 and dynamic viscosity of 1.849×10^{-5} N s/m^2.

5.2.1 Computational grid

The computational grid was composed of triangular elements and the number of these elements was of 613,135. Fig 14 shows the grid on the surface of the flying saucer.

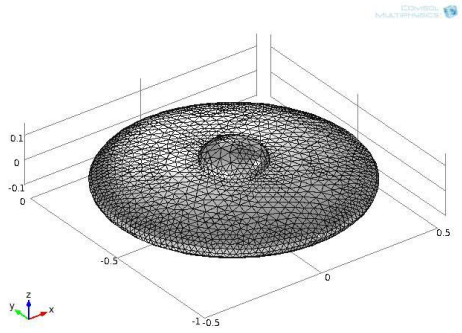

Figure 14. Surface grid

5.2.2 Results

The results obtained were: velocity field, drag and lift coefficients. The velocity field is shown in Fig 15. The drag coefficient was of 0.21934 and the lift coefficient was of 77.845×10^{-7}

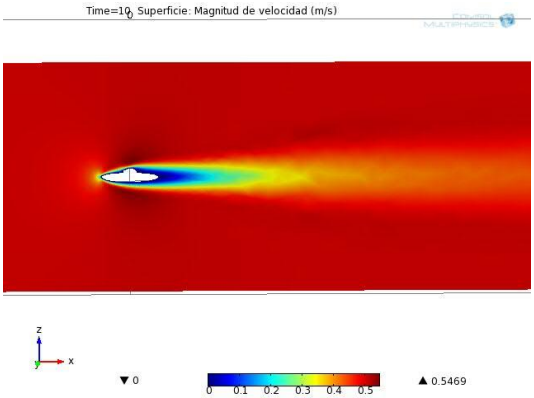

Figure 15. Velocity field in 2D. The cutting plane is located in the middle plane of the flying saucer.

6. Conclusions

The results obtained for the analyses of the flow around a cylinder and a sphere are within the range of those found in the literature, this is because the percentage error obtained for the drag coefficient is less than 8%.

Because the geometry of NAV is not a simple one, there are no references of the drag and lift coefficients; therefore, the results obtained for the simulation of the NAV with COMSOL can be considered adequate.

7. References

[1] Pruppacher, H. R.; Le Clair, B. P. and Hamielec, A. E. Some relations between drag and flow pattern of viscous flow past a sphere and a cylinder at low and intermediate Reynolds numbers. Journal of Fluid Mechanics, **(44)**:781–790. (2006).

[2] Li, J. Simulation numérique d'un écoulement bidimensionnel autour d'un et de deux cylindres en ligne par la méthode des éléments finis. PhD thesis. Université de Provence. (1989).

[3] Piñol, S. y Grau, F. Flujo alrededor de un cilindro: Efecto de la condición de contorno en la pared y de la anchura del dominio. Revista Internacional de Métodos Numéricos para Cálculo y Diseño en Ingeniería. (1996).

[4] Çengel and Cimbala, Mecánica de fluidos. Fundamentos y aplicaciones. McGraw-Hill Interamericana. (2006).

[5] Taneda, S. Experimental investigation of the wake behind sphere at low Reynolds numbers. Physical Society of Japan. (1956).

[6] Sakamoto, H. and Haniu, H. A study on vortex shedding from spheres in a uniform flow. Journal of Fluids Engineering. (1990).

[7] Defraeye, T.; Verboven, P. and Nicolai, B. (2013). CFD modeling of flow and scalar exchange of spherical food products: Turbulence and boundary-layer modeling. Journal of Food Engineering. (2013).

8. Acknowledgements

The authors express their sincere thanks to Dr. Rubén Ávila, Departamento de Termofluidos, UNAM, for the opportunity and support he gave us to realize this work with his collaboration. They also express their sincere thanks to Dr. Jaime Cervantes, Departamento de Termofluidos, UNAM, for promoting the use of COMSOL inside the Department.